Report

Current Biology

RSL Class I Genes Controlled the Development of Epidermal Structures in the Common Ancestor of Land Plants

Highlights

- Class I RSL genes control the development of structures derived from single cells
- Class I RSL function is conserved among land plants
- Class I RSL controlled epidermal development in the land plant common ancestor
- These genes controlled the development of the first plant rooting systems

Authors

Hélène Proust, Suvi Honkanen, Victor A.S. Jones, ..., Kimitsune Ishizaki, Takayuki Kohchi, Liam Dolan

Correspondence

liam.dolan@plants.ox.ac.uk

In Brief

The colonization of the land by plants was accompanied by the evolution of specialized cells and structures that develop from single cells. Proust et al. show that *RSL* class I basic helix-loop-helix transcription factors controlled the development of specialized structures from single epidermal cells in the last common ancestor of the land plants.

Proust et al., 2016, Current Biology *26*, 93–99
January 11, 2016
http://dx.doi.org/10.1016/j.cub.2015.11.042

CellPress

Current Biology
Report

RSL Class I Genes Controlled the Development of Epidermal Structures in the Common Ancestor of Land Plants

Hélène Proust,[1,4] Suvi Honkanen,[1,4] Victor A.S. Jones,[1] Giulia Morieri,[1] Helen Prescott,[1] Steve Kelly,[1] Kimitsune Ishizaki,[2] Takayuki Kohchi,[3] and Liam Dolan[1,*]
[1]Department of Plant Sciences, University of Oxford, South Parks Road, Oxford OX1 3RB, UK
[2]Graduate School of Science, Kobe University, 1-1 Rokkodai, Nada-ku, Kobe 657-8501, Japan
[3]Graduate School of Biostudies, Kyoto University, Sakyo-ku, Kyoto 606-8502, Japan
[4]Co-first author
*Correspondence: liam.dolan@plants.ox.ac.uk
http://dx.doi.org/10.1016/j.cub.2015.11.042

SUMMARY

The colonization of the land by plants, sometime before 470 million years ago, was accompanied by the evolution tissue systems [1–3]. Specialized structures with diverse functions—from nutrient acquisition to reproduction—derived from single cells in the outermost layer (epidermis) were important sources of morphological innovation at this time [2, 4, 5]. In extant plants, these structures may be unicellular extensions, such as root hairs or rhizoids [6–9], or multicellular structures, such as asexual propagules or secretory hairs (papillae) [10–12]. Here, we show that a ROOT-HAIR DEFECTIVE SIX-LIKE (RSL) class I basic helix-loop-helix transcription factor positively regulates the development of the unicellular and multicellular structures that develop from individual cells that expand out of the epidermal plane of the liverwort *Marchantia polymorpha*; mutants that lack Mp*RSL1* function do not develop rhizoids, slime papillae, mucilage papillae, or gemmae. Furthermore, we discovered that *RSL* class I genes are also required for the development of multicellular axillary hairs on the gametophyte of the moss *Physcomitrella patens*. Because class I RSL proteins also control the development of rhizoids in mosses and root hairs in angiosperms [13, 14], these data demonstrate that the function of *RSL* class I genes was to control the development of structures derived from single epidermal cells in the common ancestor of the land plants. Class I RSL genes therefore controlled the generation of adaptive morphological diversity as plants colonized the land from the water.

RESULTS AND DISCUSSION

Mutations Define a Gene Required for the Formation of Structures that Develop from Single Epidermal Cells

Unicellular rhizoids [15, 16], multicellular slime papilla [17], mucilage papillae, and gemmae (asexual propagules) [10, 18] develop from single epidermal cells that grow out of the plane of the epidermis and differentiate in the haploid phase of the life cycle in the liverwort *M. polymorpha*. To identify genes that control the development of structures derived from single epidermal cells that expand out from the epidermal surface, we identified two rhizoidless mutants, ST46-1 and ST44-8, from a population of T-DNA-transformed plants (Figures 1A, 1B, and S1A). In wild-type gemmae, rhizoids develop after approximately 24 hr from rhizoid precursor cells that are larger and paler than the surrounding epidermal cells (Figure 1E) [15]. Rhizoid precursors did not form in the gemma epidermis of either mutant ST46-1 or ST44-8 (Figures 1F and S1C), and rhizoids did not develop at any stage in the life cycle (Figures 1B, 1J, S1A, and S1D). The absence of rhizoids in ST46-1 and ST44-8 suggests that these lines are defective in genes required for rhizoid development. To determine whether the gene defective in ST46-1 and ST44-8 also controls the development of other structures derived from individual epidermal cells, we compared the development of multicellular gemmae, mucilage papillae, and slime papillae in wild-type and mutants. Both gemmae and mucilage papillae develop from individual epidermal cells located on the floor of wild-type gemma cups (Figures 1M and 1U) [10, 18]. The gemma precursor cell expands out of the plane of the epidermis and then undergoes a transverse division producing a proximal and a distal cell. The proximal cell develops as a uniseriate stalk, whereas the distal cell forms the disc-shaped multicellular gemma (Figure 1U). During mucilage papilla development, an epidermal cell swells out of the plane of the epidermal plane before dividing to form a proximal cell in the plane of the epidermis and a distal cell that swells and secretes mucilage [18]. Neither gemmae nor mucilage papillae developed in either mutant ST46-1 or ST44-8; mutant gemma cups were completely empty (Figures 1N and S1B). Whereas the epidermal surface of the floor of wild-type gemma cups was covered with cellular outgrowths (Figures 1Q and 1U), these surfaces were smooth and flat in mutants; cells did not break the plane of the epidermis (Figures 1R and 1V). This demonstrates that the activity of the wild-type gene is required for the early development of gemma and mucilage papilla precursor cells in the epidermis of the gemma cup. Slime papillae develop from single cells in the dorsal epidermis near the meristem of wild-type gemmae, where they are visible as projections from the dorsal

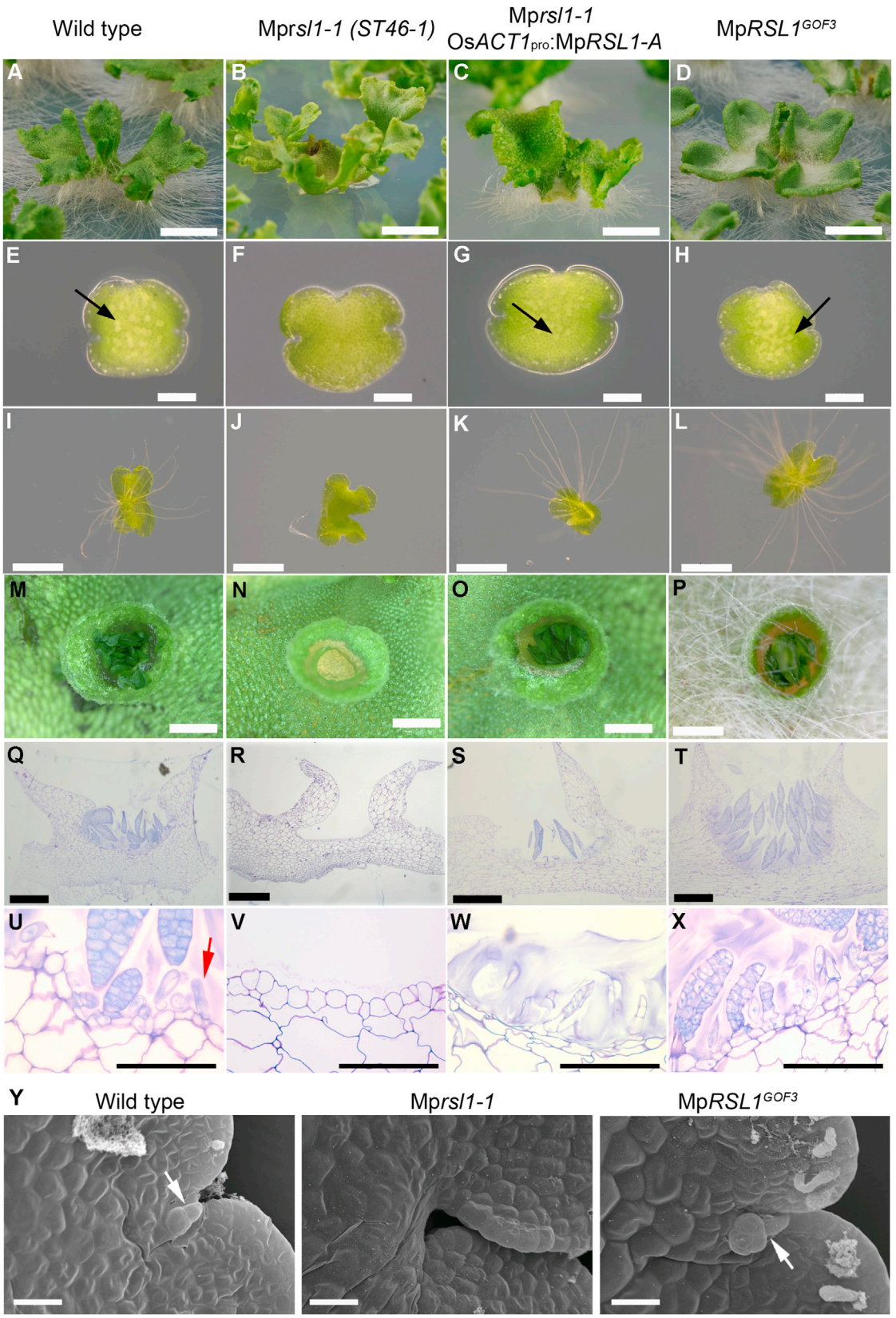

(legend on next page)

gemma epidermis (Figure 1Y) [17]. These papillae did not develop in either of ST46-1 or ST44-8 (Figure 1Y). These data demonstrate that the wild-type function of the genes defective in the ST46-1 and ST44-8 mutants is required for the development of structures—unicellular rhizoids and multicellular mucilage papillae, slime papillae, and gemmae—that are derived from individual epidermal cells in *M. polymorpha*.

Mp*RSL1* Controls the Morphogenesis of Structures Derived from Individual Epidermal Cells

To identify DNA sequence flanking each of the T-DNA insertion sites in ST46-1 and ST44-8 mutants, we carried out thermal asymmetric interlaced (TAIL) PCR using a combination of random primers and nested primers specific to the T-DNA on isolated genomic DNA [19]. The DNA sequence flanking these insertions demonstrated that the T-DNAs had inserted into intron one and exon one, respectively, of a protein-coding gene (Figures 2A and 2D; Data S1 and S2). The presence of an "RSL" motif—QLQVKVLMNDEYWP—at the carboxyl end of a basic helix-loop-helix (bHLH) domain suggested that the gene encodes a member of the *RSL* class I bHLH proteins (Figure 2B) [20]. To test this hypothesis, we constructed trees (Figures 2C and S3) using an LG maximum likelihood model [21] and approximate likelihood ratio statistics [22]. The topology of the gene tree demonstrated that MpRSL1 is a ROOTHAIR DEFECTIVE SIX-LIKE (RSL) class I basic helix-loop-helix protein (Figure 2C). Members of the RSL class I proteins are required for the development of rhizoids in the moss *P. patens* and root hairs in the angiosperm *Arabidopsis thaliana* (Figure 2C) [13, 14]. We designated the protein encoded by the gene disrupted by a T-DNA insertion in the ST46-1 and ST44-8 mutants as *M. polymorpha* ROOTHAIR SIX-LIKE1 (MpRSL1).

To determine whether the ST46-1 and ST44-8 mutant alleles resulted from loss of Mp*RSL1* function, we compared the levels of Mp*RSL1* mRNA in each mutant background with wild-type. Mp*RSL1* mRNA was not detectable in mRNA isolated from either mutant ST46-1 or ST44-8 thalli, whereas the transcript was detected in wild-type thalli (Figure 2E). This suggests that the mutant phenotype in the ST46-1 and ST44-8 lines was due to loss of Mp*RSL1* function. Therefore ST46-1 and ST44-8 were designated Mp*rsl1-1* and Mp*rsl1-2*, respectively. To verify that loss of Mp*RSL1* function is responsible for the defects in rhizoid development in these mutants, we transformed Mp*rsl1-1* thalli with the Mp*RSL1* cDNA under the transcriptional control of the rice *ACTIN1* promoter (Os$ACT1_{pro}$). Mp*RSL1* mRNA was detected in two independent Mp*rsl1-1* lines transformed with Os$ACT1_{pro}$:Mp*RSL1*, indicating that the Mp*RSL1* transgene was expressed in the transformed lines (Figure 2E). Rhizoids, mucilage papillae, and gemmae developed in both transformed lines, indicating that expression of Mp*RSL1* is sufficient to restore rhizoid (Figures 1C, 1G, and 1K), mucilage papilla, and gemma development in Mp*rsl1-1* mutant plants (Figures 1O, 1S, and 1W). These results verify that Mp*RSL1* is required for the initiation and the development of unicellular rhizoids, mucilage papillae, and gemmae in *M. polymorpha*.

To test the hypothesis that *RSL* class I genes positively regulate the development of *M. polymorpha* rhizoids, we screened T-DNA mutants for putative gain-of-function mutations in the Mp*RSL1* gene. Rhizoids do not develop on the dorsal surface of the wild-type thallus (Figure 1A). We identified five mutants in which rhizoids developed on the dorsal surface of the thallus (Figures 1D and S1E). The dorsal rhizoid phenotype segregated 1:1 after crossing each of the mutants to wild-type (Table S1), indicating that the dorsal rhizoid phenotype was caused by a single gene mutation in each line. 100% of the offspring from crosses between each of these mutants developed rhizoids on the dorsal epidermis, indicating that the mutation is in the same gene in each mutant line (Table S2). Furthermore, 100% of the mutants produced from crosses to wild-type were hygromycin resistant (Table S1). This indicates that a T-DNA was closely linked to the rhizoid mutation in each of these mutants. To identify the genomic DNA sequences flanking each of the T-DNAs in these five dorsal rhizoid mutants, we carried out TAIL PCR using a combination of random primers and nested primers in the T-DNA [19]. The flanking sequences demonstrated that T-DNAs were inserted 1.6 kb, 2.6 kb, 6 kb, 14.5 kb, and 15 kb upstream (5′) of the start codon of the Mp*RSL1* gene in these mutants (Figures 2A and 2F; Data S1 and S2). Steady-state levels of Mp*RSL1* mRNA were higher in each mutant than in wild-type (Figure 2G). These data demonstrate that the insertion of the T-DNA in the 5′ region of the gene results in higher steady-state levels of Mp*RSL1* mRNA. These mutant lines were therefore designated Mp$RSL1^{GOF1}$, Mp$RSL1^{GOF2}$, Mp$RSL1^{GOF3}$, Mp$RSL1^{GOF4}$, and Mp$RSL1^{GOF5}$, respectively (where GOF indicates that these are gain-of-function mutations). The demonstration that supernumerary rhizoids develop on Mp*RSL1* gain-of-function mutants and rhizoids do not develop on Mp*rsl1* loss-of-function mutants indicates that Mp*RSL1* positively regulates rhizoid development. These data also demonstrate that Mp*RSL1* is sufficient for rhizoid development. Ectopic slime papillae (Figure 1Y), mucilage papillae, and gemmae (Figures 1P, 1T, and 1X) did not develop in the Mp*RSL1* gain-of-function mutants. This suggests that whereas Mp*RSL1* function is sufficient for rhizoid development, it is most likely not sufficient for slime papilla, mucilage papilla, or gemma development.

Figure 1. Mp*RSL1* Positively Regulates the Initiation of Rhizoids, Gemmae, Mucilage Papillae, and Slime Papillae in *M. polymorpha*

(A–X) Four genotypes are presented, one in each column: (first column) wild-type, (second column) Mp*rsl1-1* mutants, (third column) Mp*rsl1-1* Os$ACT1_{pro}$:Mp*RSL1-A*, and (fourth column) Mp$RSL1^{GOF3}$. Six different stages are presented in rows.

(A–D) Rhizoids on 28-day-old thalli grown from gemmae. Scale bars represent 1 cm.

(E–H) Zero-day-old gemmae. Arrows highlight the position of pale rhizoid precursor cells. Scale bars represent 200 μm.

(I–L) Rhizoids developing on 4-day-old gemmae. Scale bars represent 1 mm.

(M–P) Surface view of gemma cups of 1-month-old plant. Scale bars represent 1 mm.

(Q–T) Toluidine-blue-stained longitudinal sections of gemma cups in a 1-month-old plant. Scale bars represent 500 μm.

(U–X) Toluidine-blue-stained longitudinal sections of gemma cups in a 1-month-old plant. The red arrow indicates a mucilage papilla; the black arrow indicates a gemma primordium. Scale bars represent 100 μm.

(Y) Wild-type, Mp*rsl1-1*, and Mp$RSL1^{GOF3}$ 1-day-old gemmae. Arrows indicate slime papillae. Scale bars represent 20 μm.

See also Figure S1.

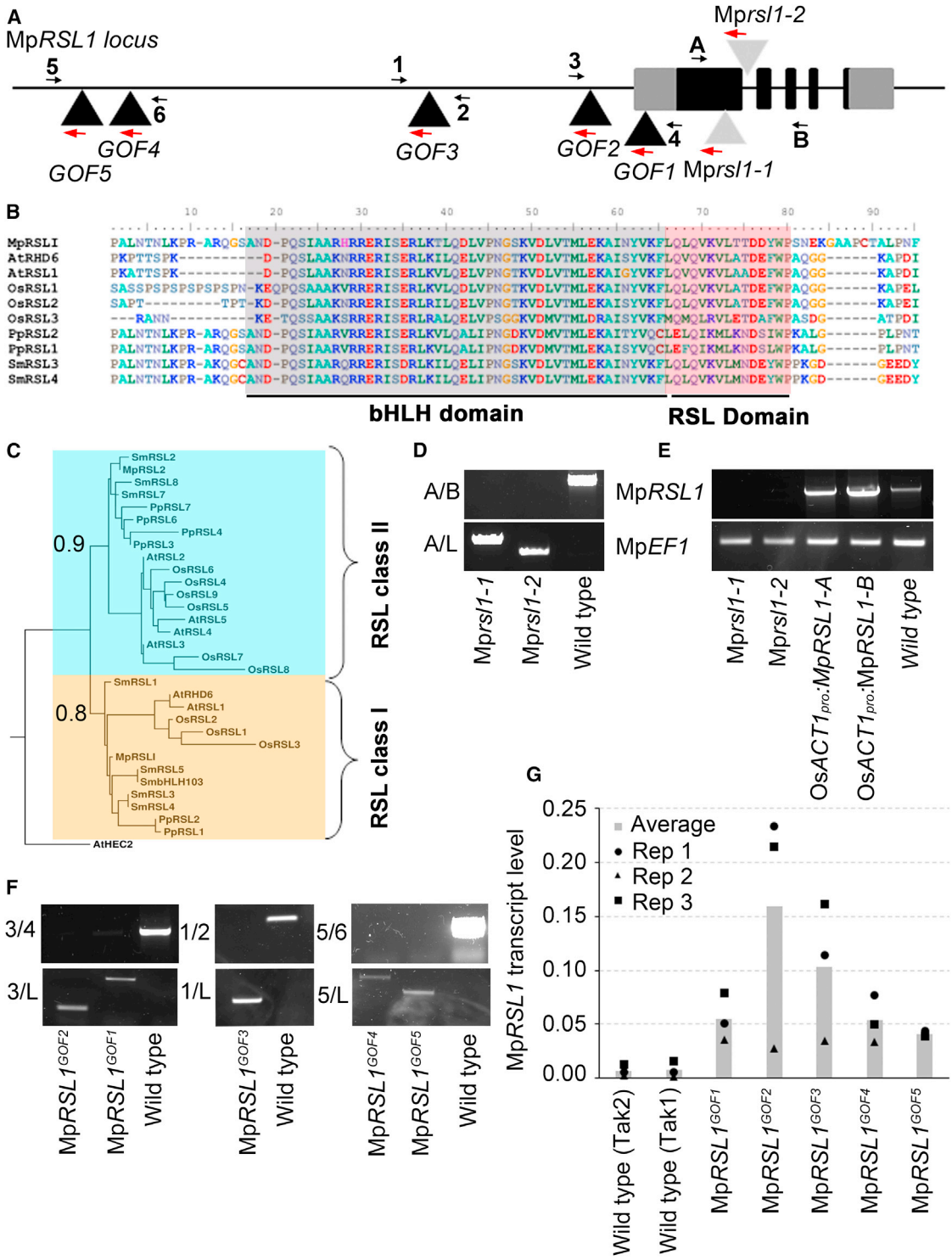

Figure 2. Molecular Characterization of Mp*rsl1* Loss-of-Function and Mp*RSL1*^{GOF} Mutations

(A) Schematic of Mp*RSL1* gene structure. Black and gray boxes represent exons of CDS and UTR of Mp*RSL1*, respectively. Black and light gray triangles indicate the T-DNA insertion site in each Mp*RSL1*^{GOF} and Mp*rsl1* loss-of-function line, respectively.

(B) Alignment of land plant RSL class I proteins. bHLH and RSL domains are highlighted in gray and red, respectively.

(C) A maximum-likelihood tree of RSL class I (yellow box) and RSL class II proteins (blue box) rooted with AtHEC2. Bootstrap values are indicated at the nodes.

(D) Amplification of Mp*rsl1-1* and Mp*rsl1-2* T-DNA insertion site from genomic DNA. A and B are Mp*RSL1* locus-specific primers, and L is a T-DNA left-border-specific primer.

(legend continued on next page)

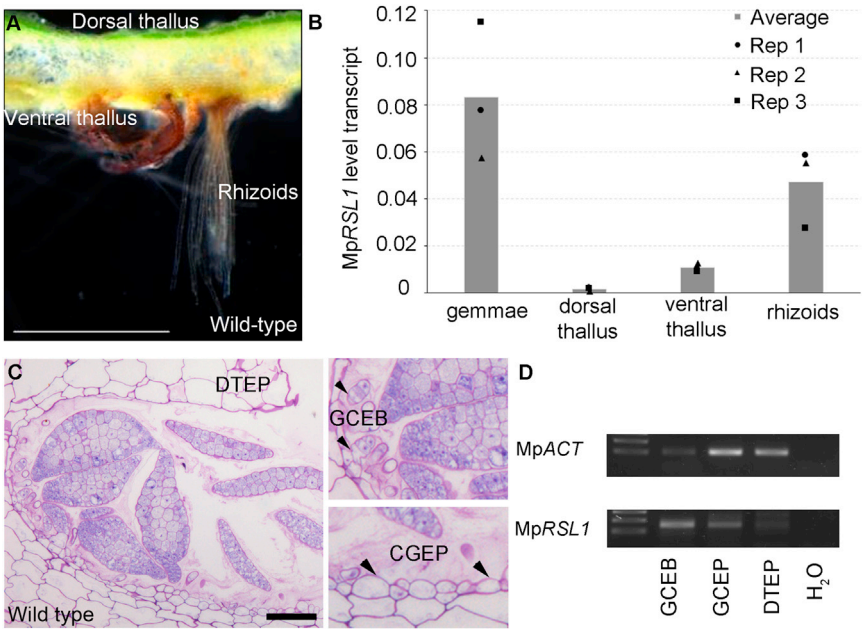

Figure 3. Mp*RSL1* Is Expressed in Rhizoid and Gemma Precursor Cells

(A and B) Expression of Mp*RSL1* in different tissues of 1-month-old wild-type gemmalings.

(A) Cross-section of 1-month-old wild-type thallus showing dorsal and ventral thallus and rhizoid.

(B) Analysis of Mp*RSL1* level transcript by qRT-PCR. Histograms represent the mean transcript levels (n = 3) normalized with the geometric mean of Mp*EF1* and Mp*CUL* transcript level in different organs. The three biological replicates are represented with circle, triangle, and square for replicate 1, replicate 2, and replicate 3, respectively.

(C and D) Expression of Mp*RSL1* in gemmae primordia.

(C) Toluidine-blue-stained cross-section of a gemma cup showing gemma buds (GCEB), gemma cup epidermis cells (GCEP), and thallus epidermis cells (DTEP). The two small pictures are magnification of the first picture. The scale bar represents 200 μm.

(D) Analysis by semi-qRT-PCR of Mp*RSL1* level transcript in gemma buds (GCEB), gemma cup epidermis cells (GCEP), and thallus epidermis cells (DTEP). Mp*ACT* was used as reference gene.

See also Figure S3.

MpRSL1 Is Expressed in Epidermal Cells that Form Specialized Structures

We predicted that Mp*RSL1* would be expressed in epidermal cells that swell and break the plane of the epidermis during morphogenesis. We measured steady-state levels of Mp*RSL1* mRNA in isolated cells and tissues and found expression in rhizoids (Figures 3A and 3B). Mp*RSL1* transcript was also detected in gemmae and ventral thallus, where rhizoids develop. In contrast, no significant Mp*RSL1* mRNA transcript was detected in the cells of the mature dorsal thallus where epidermal cells that break the epidermal plane do not develop. To determine when Mp*RSL1* is first expressed in cells that break the epidermal plane during their development, we carried out semi-qRT-PCR analysis on mRNA isolated from single cells of the epidermis inside the gemma cup where mucilage papillae and gemmae develop using laser capture microdissection (Figure S3). RNA was isolated from epidermal cells that had expanded out of the plane of the epidermis to form buds (GCEB) inside the gemma cup, epidermal cells from the inside of the of the gemma cup that were not forming outgrowths (GCEP), and dorsal thallus epidermal cells (DTEP) in which growth out of the epidermal plane does not occur (Figures 3C and S3A–S3C). Mp*RSL1* mRNA was detectable in the bud cells (GCEB), was less abundant in the epidermal cells that do not break the plane of the epidermis (GCEP), and was not detectable in the cells of the dorsal thallus epidermis from which epidermis-derived structures do not develop (DTEP) (Figures 3D and S3). This indicates that Mp*RSL1* is expressed in cells that swell out of the epidermal plane during the formation of rhizoids, mucilage papillae, and gemmae. Taken together, these data indicate that Mp*RSl1* is expressed in the cells that expand out of the epidermis and subsequently form unicellular and multicellular structures in *M. polymorpha*.

RSL Class I Function Is Conserved in Land Plants

To determine whether *RSL* class I genes control the development of cells that break the plane of the epidermis in other taxa, we characterized the development of epidermis-derived structures in the Pp*rsl1* Pp*rsl2* double mutant of the moss *P. patens*. We previously showed that rhizoid development was defective in Pp*rsl1* Pp*rsl2* double mutants [13, 14]. To determine whether these genes control the development of other structures derived from individual epidermal cells, we compared the development of the multicellular hairs that develop in the axils of leaves [23] on wild-type and Pp*rsl1* Pp*rsl2* double mutants (Figures 4A and 4B). Whereas wild-type developed between one and two axillary hairs per node (1.45 ± 0.57 hairs per axil), Pp*rsl1* Pp*rsl2* double mutants developed 0.47 (±0.3) hairs per axil (Student's t test indicates that these means are different at $p < 0.0001$). This demonstrates that *RSL* class I genes control

(E) RT-PCR analysis of the presence or absence of Mp*RSL1* full-length cDNA in the Mp*rsl1-1* and Mp*rsl1-2* loss-of-function mutants, two Mp*rsl1-1* loss of function complemented with $OsACT_{pro}$:Mp*RSL1* lines, and wild-type. Mp*EF1* is a reference gene.

(F) Amplification of Mp$RSL1^{GOF1}$ -Mp$RSL1^{GOF5}$ T-DNA insertion site with Mp*RSL1* promoter-specific primers flanking the insertion site (top) and with an Mp*RSL1* promoter-specific primer and a T-DNA left-border-specific primer (bottom). Amplification was performed on genomic DNA. Primers 1–6 are Mp*RLS1* promoter-specific primers. L is a T-DNA left-border-specific primer.

(G) Analysis by qRT-PCR of Mp*RSL1* expression in the different Mp$RSL1^{GOF}$ mutants. Histograms represent the average Mp*RSL1* transcript levels (n = 3) normalized with the geometric mean of Mp*EF1* and Mp*CUL* transcript levels. The three biological replicates are represented with circle, triangle, and square for replicate 1, replicate 2, and replicate 3, respectively.

See also Figure S2, Data S1 and S2, and Tables S1 and S2.

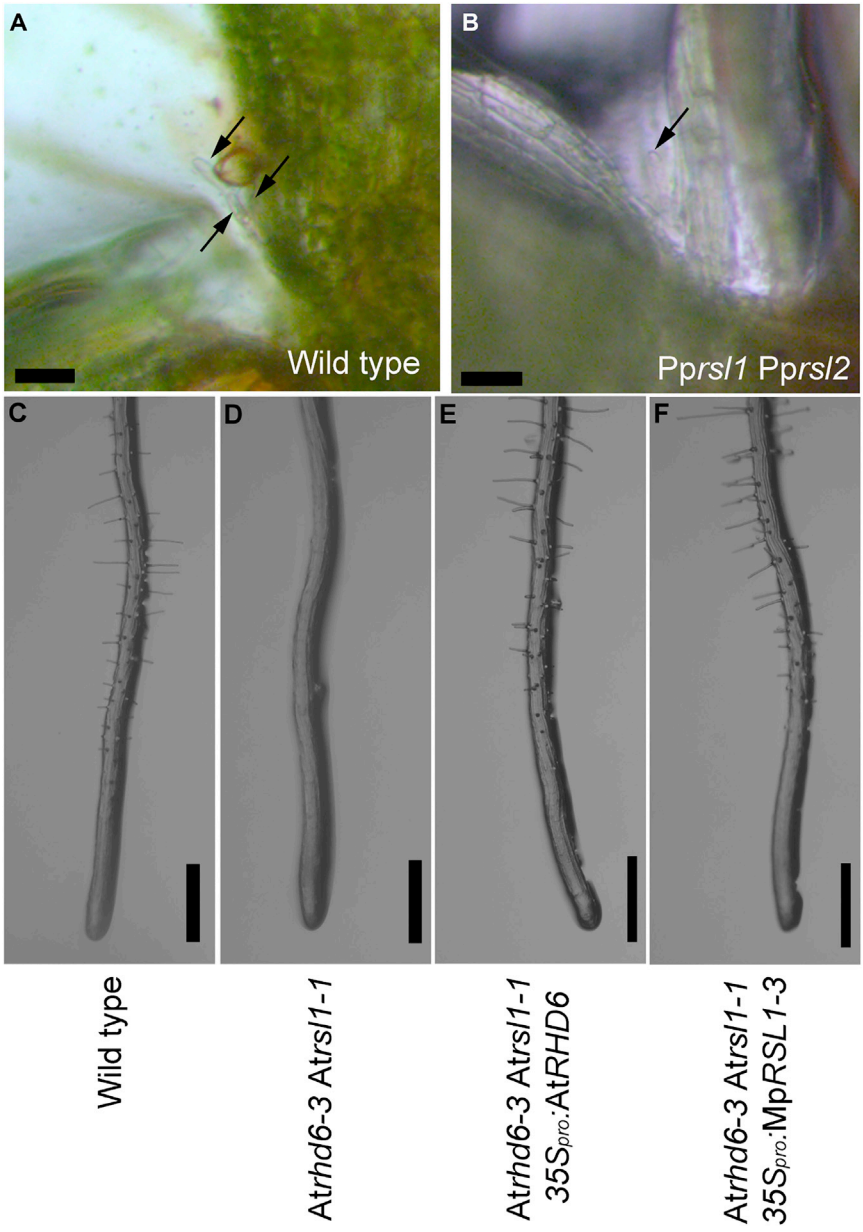

Figure 4. The Function of RSL Class I Proteins in the Formation of Structures that Develop from Individual Epidermal Cells Has Been Conserved Among Land Plants

(A and B) Papillae on *P. patens* gametophores from 1-month-old colonies. Arrows highlight axillary papillae. The scale bar represents 50 μm.

(A) More than one slime papilla develops at each node on wild-type gametophores (arrows).

(B) One or no slime papilla develops at each node of Pp*rsl1* Pp*rsl2* double mutant gametophores. The arrow identifies the single papilla that develops at a node of the Pp*rsl1* Pp*rsl2* double mutant.

(C–F) Five-day-old seedlings of *A. thaliana*. The scale bar represents 500 μm.

(C) Wild-type (with root hairs).

(D) *Atrhd6-3 Atrsl1-1* double mutant (root hairless).

(E and F) *Atrhd6-3* At*rsl1-1* double mutant transformed with $35S_{pro}$:At*RHD6* (with root hairs) (E) and At*rhd6-3* At*rsl1-1* double mutant transformed with $35S_{pro}$:Mp*RSL1* (F).

See also Figure S4.

the development of structures—rhizoids and axillary hairs—derived from single cells that break the epidermal plane during development in mosses.

We previously demonstrated that *RSL* class I genes control root hairs in *A. thaliana* [13]. To determine whether the molecular function of *RSL* class I genes has diverged since evolving from the *RSL* class I gene in the common ancestor of extant land plants, we tested whether the Mp*RSL1* gene could program the development of root hairs in *A. thaliana* mutants plants devoid of *RSL* class I gene function (At*rhd6* At*rsl1* double mutants). Whereas root hairs do not develop in At*rhd6* At*rsl1* double mutants (Figures 4C and 4D), root hairs develop on At*rhd6* At*rsl1* double mutants transformed with Mp*RSL1* (Figures 4E and S4). These plants are identical to plants transformed with the *RSL* class I gene from *A. thaliana*, At*RHD6* (Figure 4F). Whereas 81% of the amino acids are identical in the bHLH-RSL domains of MpRSL1 and AtRHD6, there is no conservation elsewhere in the protein. This demonstrates that, despite sequence divergence, the molecular function of RSL class I proteins has not diverged since *M. polymorpha* and *A. thaliana* last shared a common ancestor more than 470 million years ago.

A diversity of structures in land plants—unicellular rhizoids and root hairs to multicellular organs such as gemmae—develop from single cells in the epidermis [6, 15–18]. Early in development, individual cells change their growth polarity and expand perpendicular to the plane of the epidermal surface to form balloon-shaped swellings. Tip growth may initiate from these outgrowths during the differentiation of rhizoids and root hairs. Alternatively, the swollen cell may divide once or many times to form multicellular structures and organs, such as gemmae and slime papillae. We discovered that the *RSL* class I mechanism is required for the development of a variety of cells that develop from cells that break the epidermal plane before undergoing morphogenesis in liverworts, mosses, and angiosperms. The conserved role of class I *RSL* genes in development of structures developing from single epidermal cells that break the plane of the epidermis suggests that these genes controlled this process in the common ancestor of all land plants. Given that many epidermal structures develop from single epidermal cells that expand beyond the surface plane of the epidermis prior to differentiation and organogenesis, our data demonstrate that *RSL* class I genes played an important role in the generation of cellular and organ diversity in the newly evolved epidermis early in land plant evolution. Many of these

structures were key adaptations to life on land—protecting the plant and plant parts from desiccation and providing access to inorganic nutrients [1, 3, 24]. Therefore, the evolution of the *RSL* class I mechanism allowed the generation of morphological diversity that facilitated adaptation of green plants to life in the terrestrial environment as plants colonized the land from the water.

ACCESSION NUMBERS

The accession numbers for the Mp*RSL1* and Mp*RSL2* sequences reported in this paper are Genbank: KT633827 and Genbank: KT633828, respectively.

SUPPLEMENTAL INFORMATION

Supplemental Information includes Supplemental Experimental Procedures, four figures, two tables, and two data files and can be found with this article online at http://dx.doi.org/10.1016/j.cub.2015.11.042.

AUTHOR CONTRIBUTIONS

H. Proust performed the experiments and analyzed the data with L.D. S.H. isolated lines with gain-of-function and loss-of-function mutations and identified insertions sites; V.A.S.J. and G.M. isolated lines with gain-of-function mutations and identified insertions sites. H. Proust, G.M., and S.K. isolated and sequenced mRNA and analyzed the transcriptomes and the genome of *M. polymorpha*. K.I. and T.K. provided Mp*RSL1* sequences at the start of the project. H. Prescott initiated the transformation and establishment of the *Marchantia* system in the lab. H. Proust and L.D. designed the experiments and wrote the paper. L.D. conceived and supervised the project.

ACKNOWLEDGMENTS

This research was funded by the EVO500 ERC AdG award to L.D. and a JSPS Fellowship for Overseas Researchers (short-term: PE12565) award to H. Proust held with T.K. We are grateful to Dr. Chulmin Kim, Dr. Denis Saint-Marcoux, Dr. Clémence Bonnot, Bruno Catarino, and Sandy Hetherington for helpful discussions. We are grateful to Bruno Catarino for his help with the phylogenetic analysis. We are grateful to Dr. Denis Saint-Marcoux for his help for the laser microdissection experiments. We would like to thank Dr. Keke Yi for providing the *Arabidopsis thaliana* line transformed with the *35S*:At*RHD6* construct.

Received: October 7, 2015
Revised: November 5, 2015
Accepted: November 6, 2015
Published: December 24, 2015

REFERENCES

1. Kenrick, P., and Crane, P.R. (1997). The origin and early evolution of plants on land. Nature *389*, 33–39.
2. Ligrone, R., Duckett, J.G., and Renzaglia, K.S. (2012). Major transitions in the evolution of early land plants: a bryological perspective. Ann. Bot. *109*, 851–871.
3. Doyle, J.A. (2013). Phylogenetic analyses and morphological evolution in land plants. In Annual Plant Reviews Volume 45: The Evolution of Plant Form, B.A. Ambrose, and M. Purugganan, eds. (John Wiley and Sons), pp. 1–50.
4. Ramsay, N.A., and Glover, B.J. (2005). MYB-bHLH-WD40 protein complex and the evolution of cellular diversity. Trends Plant Sci. *10*, 63–70.
5. Goffinet, B., and Buck, W.R. (2013). The evolution of body form in bryophytes. In Annual Plant Reviews Volume 45: The Evolution of Plant Form, B.A. Ambrose, and M. Purugganan, eds. (John Wiley and Sons), pp. 51–90.
6. Carol, R.J., and Dolan, L. (2002). Building a hair: tip growth in Arabidopsis thaliana root hairs. Philos. Trans. R. Soc. Lond. B Biol. Sci. *357*, 815–821.
7. Alfano, F., Russell, A., Gambardella, R., and Duckett, G. (1993). The actin cytoskeleton of the liverwort *Riccia fluitans*: effects of cytochalasin B and aluminum ions on rhizoid tip growth. J. Plant Physiol. *142*, 569–574.
8. Pressel, S., Ligrone, R., and Duckett, J.G. (2008). Cellular differentiation in moss protonemata: a morphological and experimental study. Ann. Bot. *102*, 227–245.
9. Jones, V.A., and Dolan, L. (2012). The evolution of root hairs and rhizoids. Ann. Bot. *110*, 205–212.
10. Barnes, C.R., and Land, W.J.G. (1908). Bryological papers. II. The origin of the cupule of *Marchantia*. Bot. Gaz. *46*, 401–409.
11. Duckett, J.G., and Ligrone, R. (1995). The formation of catenate foliar gemmae and the origin of oil bodies in the liverwort *Odontoschisma denudatum* (Mart.) Dum. (Jungermanniales): a light and electron microscope study. Ann. Bot. *76*, 405–419.
12. Ligrone, R., Duckett, J.G., and Gambardella, R. (1996). Serial development of foliar gemmae in *Tortula* (Pottiales, Musci), an ultrastructural study. Ann. Bot. *78*, 305–315.
13. Menand, B., Yi, K., Jouannic, S., Hoffmann, L., Ryan, E., Linstead, P., Schaefer, D.G., and Dolan, L. (2007). An ancient mechanism controls the development of cells with a rooting function in land plants. Science *316*, 1477–1480.
14. Jang, G., Yi, K., Pires, N.D., Menand, B., and Dolan, L. (2011). RSL genes are sufficient for rhizoid system development in early diverging land plants. Development *138*, 2273–2281.
15. Tarén, N. (1958). Factors regulating the initial development of gemmae in Marchantia polymorpha. Bryologist *61*, 191–204.
16. Cao, J.-G., Dai, X.-L., Zou, H.-M., and Wang, Q.-X. (2014). Formation and development of rhizoids of the liverwort *Marchantia polymorpha*. J. Torrey Bot. Soc. *141*, 126–134.
17. Renzaglia, K.S., Duff, R.J.T., Nickrent, D.L., and Garbary, D.J. (2000). Vegetative and reproductive innovations of early land plants: implications for a unified phylogeny. Philos. Trans. R. Soc. Lond. B Biol. Sci. *355*, 769–793.
18. Vashishta, B.R., Sinha, A.K., and Kumar, A. (2011). Botany for Degree Students Part III: Bryophyta (S. Chand).
19. Ishizaki, K., Chiyoda, S., Yamato, K.T., and Kohchi, T. (2008). Agrobacterium-mediated transformation of the haploid liverwort *Marchantia polymorpha L.*, an emerging model for plant biology. Plant Cell Physiol. *49*, 1084–1091.
20. Pires, N., and Dolan, L. (2010). Origin and diversification of basic-helix-loop-helix proteins in plants. Mol. Biol. Evol. *27*, 862–874.
21. Le, S.Q., and Gascuel, O. (2008). An improved general amino acid replacement matrix. Mol. Biol. Evol. *25*, 1307–1320.
22. Anisimova, M., and Gascuel, O. (2006). Approximate likelihood-ratio test for branches: A fast, accurate, and powerful alternative. Syst. Biol. *55*, 539–552.
23. Eklund, D.M., Thelander, M., Landberg, K., Ståldal, V., Nilsson, A., Johansson, M., Valsecchi, I., Pederson, E.R., Kowalczyk, M., Ljung, K., et al. (2010). Homologues of the Arabidopsis thaliana SHI/STY/LRP1 genes control auxin biosynthesis and affect growth and development in the moss Physcomitrella patens. Development *137*, 1275–1284.
24. Langdale, J.A. (2008). Evolution of developmental mechanisms in plants. Curr. Opin. Genet. Dev. *18*, 368–373.

Current Biology

Supplemental Information

RSL Class I Genes Controlled the Development of Epidermal Structures in the Common Ancestor of Land Plants

Hélène Proust, Suvi Honkanen, Victor A.S. Jones, Giulia Morieri, Helen Prescott, Steve Kelly, Kimitsune Ishizaki, Takayuki Kohchi, and Liam Dolan

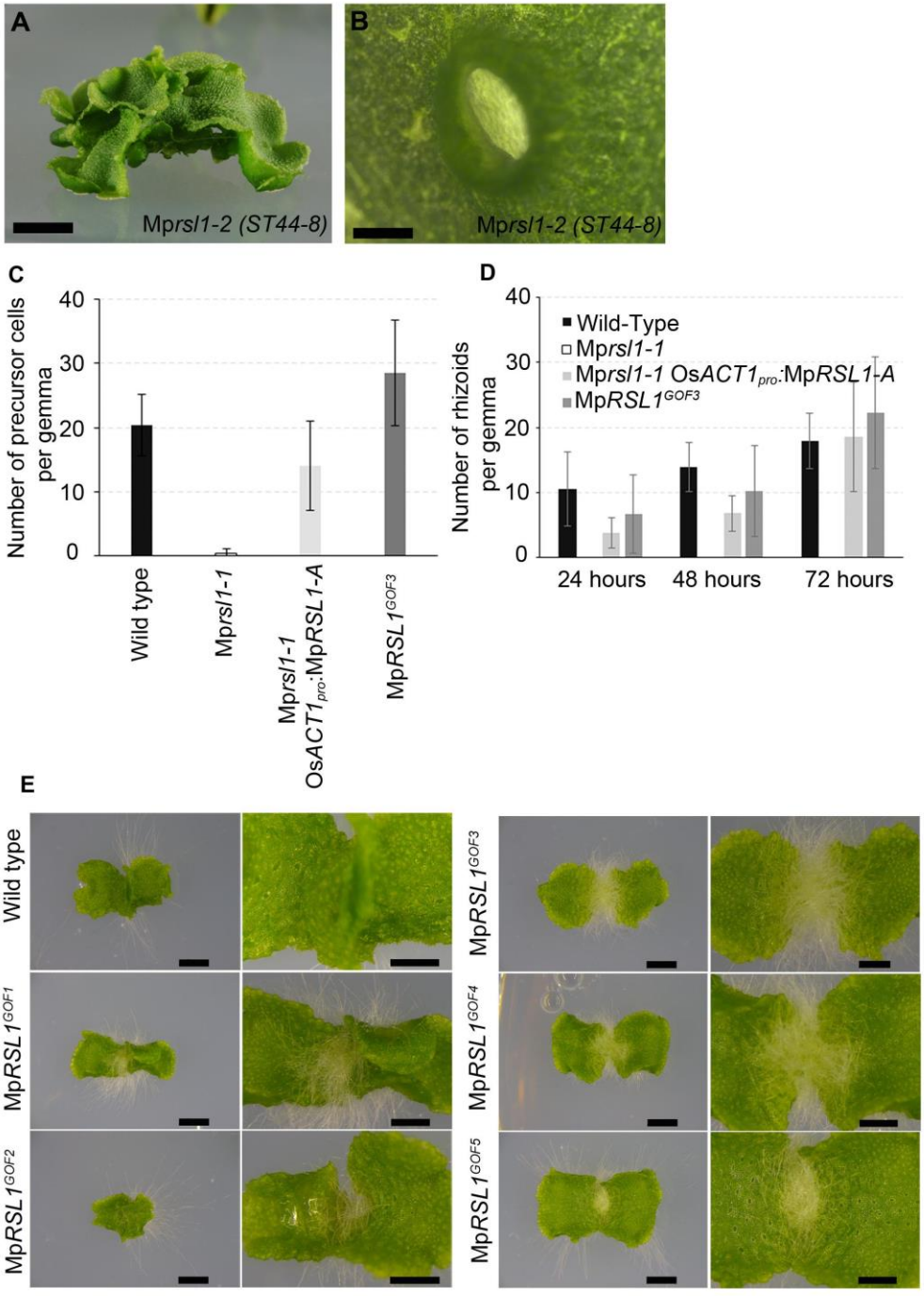
A
Mprsl1-2 (ST44-8)
B
Mprsl1-2 (ST44-8)
C
Number of precursor cells per gemma
40
30
20
10
0
Wild type
Mprsl1-1
Mprsl1-1 OsACT1pro:MpRSL1-A
MpRSL1GOF3
D
Number of rhizoids per gemma
40
30
20
10
0
Wild-Type
Mprsl1-1
Mprsl1-1 OsACT1pro:MpRSL1-A
MpRSL1GOF3
24 hours
48 hours
72 hours
E
Wild type
MpRSL1GOF1
MpRSL1GOF2
MpRSL1GOF3
MpRSL1GOF4
MpRSL1GOF5

Figure S1

Figure S1, related to figure 1

Mp*rsl1* and Mp*RSL1*^{GOF} lines phenotype.

(A) Rhizoids do not develop in 1 month-old Mp*rsl1-2* (ST44-8) plants. Bar, 1 cm.

(B) Gemmae do not develop in Mp*rsl1-2* gemma cups. Bar, 1 mm.

(C) Number of rhizoid precursors in wild type, Mp*rsl1-1*, Mp*rsl1-1* Os*ACT1*$_{pro}$*:*Mp*RSL1-A*, and Mp*RSL1*^{GOF3} 0 day-old gemmae.

(D) The histograms represent the mean (± SD) number of rhizoid precursor cells on 0 days-old gemmae, n=20. Rhizoid number in wild type, Mp*rsl1-1*, Mp*rsl1-1* Os*ACT1*$_{pro}$*:*Mp*RSL1-A*, Mp*RSL1*^{GOF3} 4-day-old gemmae. The histograms represent the average (+/- SD) of number of rhizoids per 4-days-old gemmalings in different lines, n=20.

(E) 15-days-old gemmalings of wild type (Tak 1), Mp*RSL1*^{GOF1}, MpRSL1^{GOF2}, Mp*RSL1*^{GOF3}, Mp*RSL1*^{GOF4} and Mp*RSL1*^{GOF5}. Scales bar: right panel, 2 mm; left panel, 1mm.

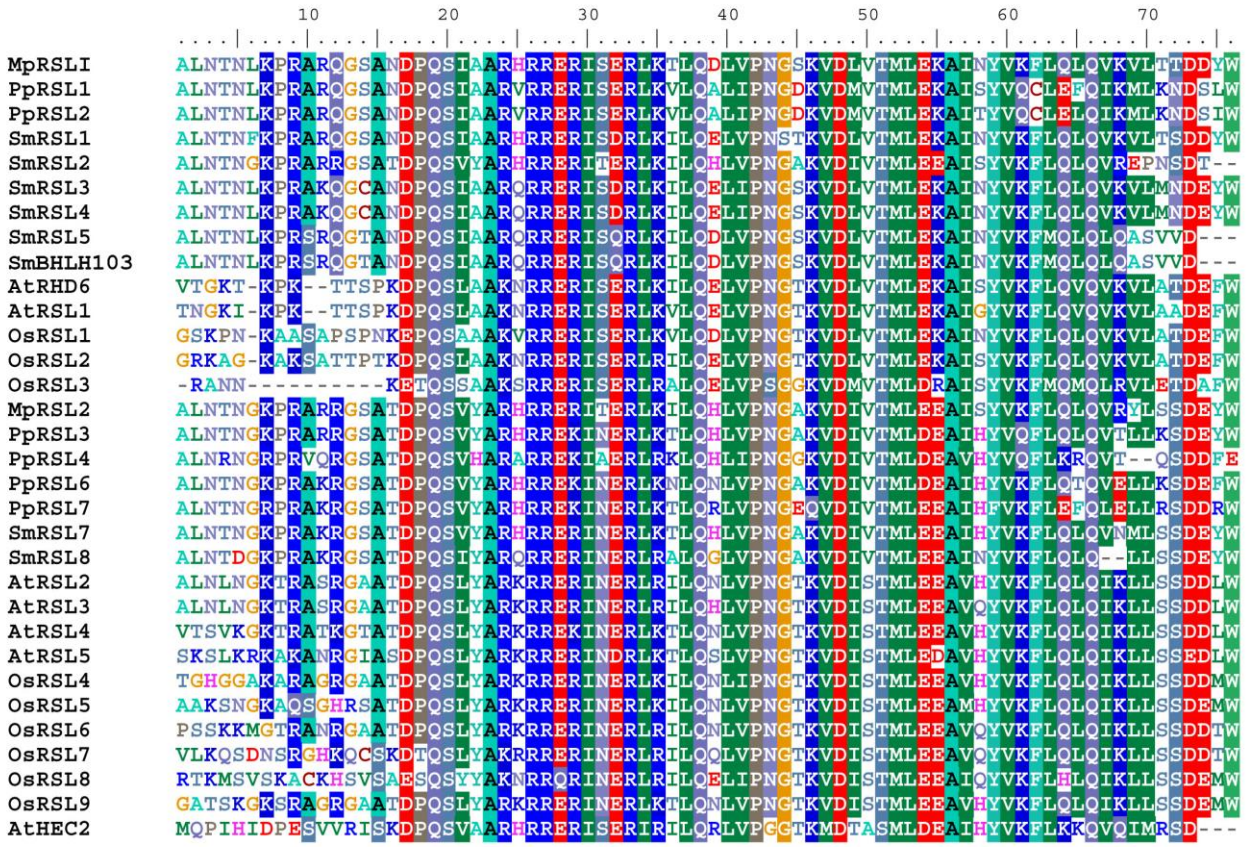
10
20
30
40
50
60
70
MpRSLI
PpRSL1
PpRSL2
SmRSL1
SmRSL2
SmRSL3
SmRSL4
SmRSL5
SmBHLH103
AtRHD6
AtRSL1
OsRSL1
OsRSL2
OsRSL3
MpRSL2
PpRSL3
PpRSL4
PpRSL6
PpRSL7
SmRSL7
SmRSL8
AtRSL2
AtRSL3
AtRSL4
AtRSL5
OsRSL4
OsRSL5
OsRSL6
OsRSL7
OsRSL8
OsRSL9
AtHEC2

Figure S2

Figure S2, related to figure 2

Alignment of RSL Class I (pink box), RSL Class II (blue box) and AtHEC2 protein used for the construction of the maximum likelihood tree.

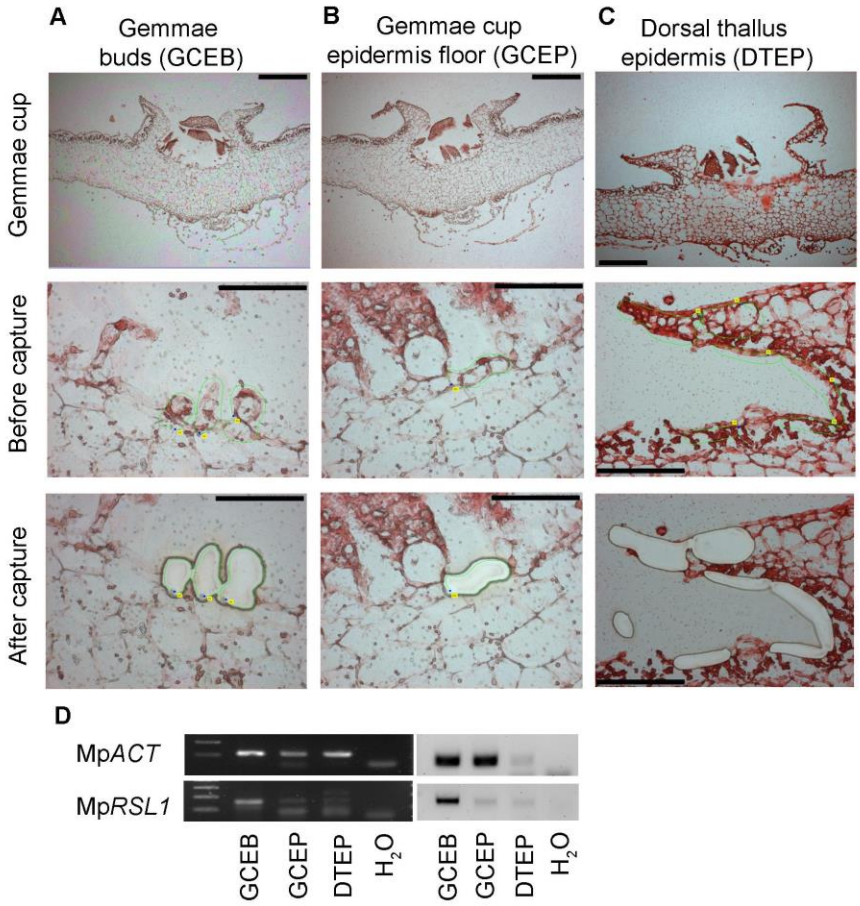
A
Gemmae buds (GCEB)
B
Gemmae cup epidermis floor (GCEP)
C
Dorsal thallus epidermis (DTEP)
Gemmae cup
Before capture
After capture
D
MpACT
MpRSL1
GCEB
GCEP
DTEP
H2O
GCEB
GCEP
DTEP
H2O

Figure S3

Figure S3, related to figure 3

Mp*RSL1* transcript levels in cells captured by laser microdissection.

(A) gemma cup epidermal buds, (B) gemma cup epidermal cells and (C) dorsal thallus epidermal cells before dissection (top and middle panel) and after capture (bottom panel). Bar: top panel, 300 µm; middle and bottom panel, 75 µm.

(D) RT-PCR analysis of Mp*RSL1* transcript level in gemma cup epidermal buds (GCEB), gemmae cup epidermal cells (GCEP) and thallus epidermal cells (DTEP). Mp*ACT* was used as reference gene.

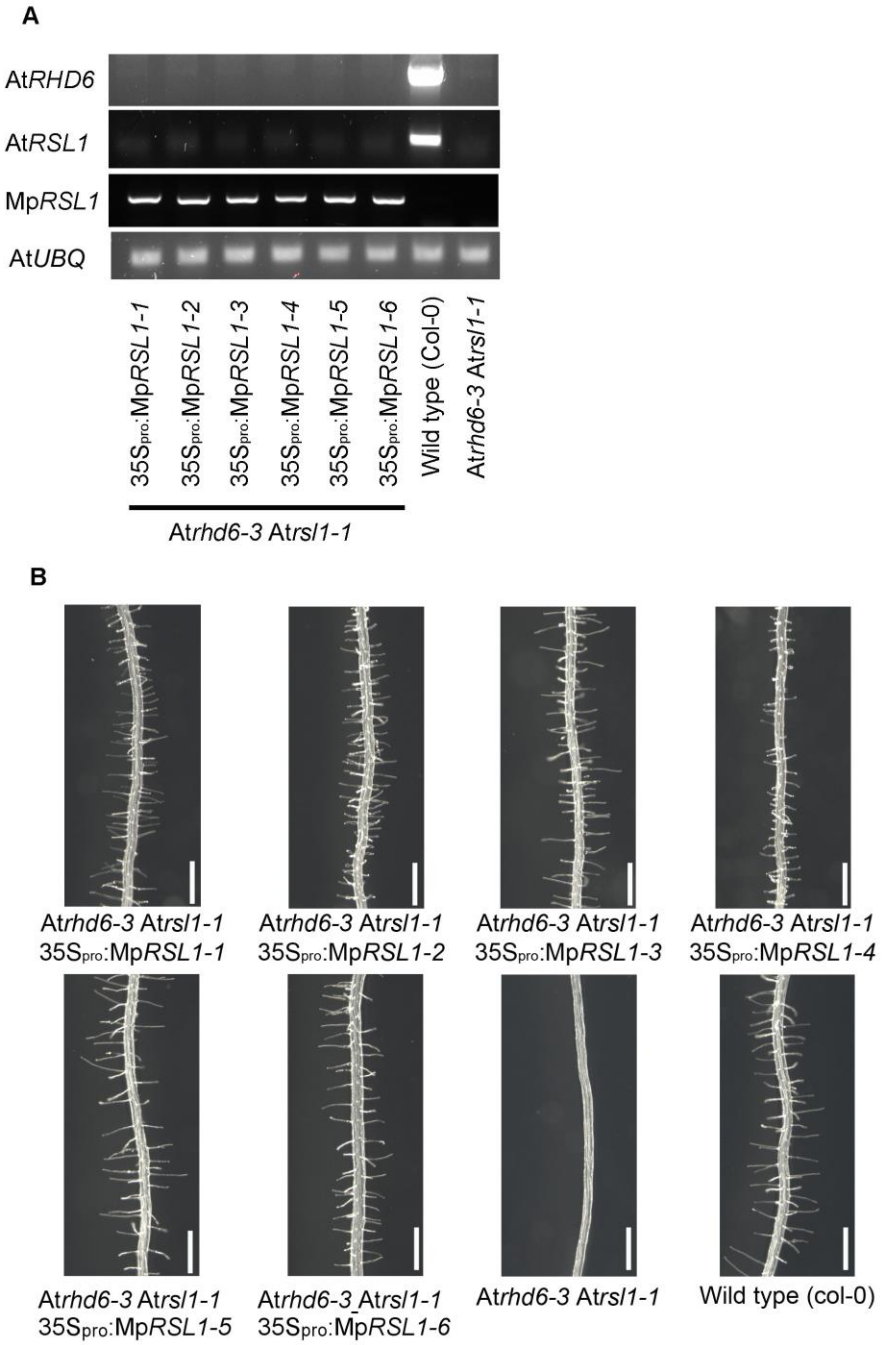
A
AtRHD6
AtRSL1
MpRSL1
AtUBQ
35Spro:MpRSL1-1
35Spro:MpRSL1-2
35Spro:MpRSL1-3
35Spro:MpRSL1-4
35Spro:MpRSL1-5
35Spro:MpRSL1-6
Wild type (Col-0)
Atrhd6-3 Atrsl1-1
Atrhd6-3 Atrsl1-1
B
Atrhd6-3 Atrsl1-1 35Spro:MpRSL1-1
Atrhd6-3 Atrsl1-1 35Spro:MpRSL1-2
Atrhd6-3 Atrsl1-1 35Spro:MpRSL1-3
Atrhd6-3 Atrsl1-1 35Spro:MpRSL1-4
Atrhd6-3 Atrsl1-1 35Spro:MpRSL1-5
Atrhd6-3 Atrsl1-1 35Spro:MpRSL1-6
Atrhd6-3 Atrsl1-1
Wild type (col-0)

Figure S4

Figure S4, related to figure 4

Expression of Mp*RSL1* restores root hair development in the root hairless At*rhd6-3* At*rsl1-1* double mutant.

(A) Semi-quantitative RT-PCR analysis of At*RHD6*, At*RSL1* and Mp*RSL1* expression in Wild type (Col-0), At*rhd6-3* At*rsl1-1* double mutant and At*rhd6-3* At*rsl1-1* double mutants transformed with $35S_{pro}$:Mp*RSL1*.

(B) Root hair phenotype of At*rhd6-3* At*rsl1-1* double mutants, At*rhd6-3* At*rsl1-1* 3$5S_{pro}$:Mp*RSL1-1*, At*rhd6-3* At*rsl1-1* $35S_{pro}$:Mp*RSL1-2*, At*rhd6-3* At*rsl1-1* $35S_{pro}$:Mp*RSL1-3*, At*rhd6-3* At*rsl1-1* $35S_{pro}$:Mp*RSL1-4*, At*rhd6-3* At*rsl1-1* $35S_{pro}$:Mp*RSL1-5*, At*rhd6-3* At*rsl1-1* $35S_{pro}$:Mp*RSL1-6*. Bar: 500 µm.

Table S1, related to figure S2

Mp*RSL1*^{GOF} lines possess a single T-DNA insertion.

	Mutant phenotype		Wild-Type phenotype		
	HygR	HygS	HygR	HygS	T-DNA insertion
Mp*RSL1*^{GOF1}	106	0	0	123	1
Mp*RSL1*^{GOF2}	108	0	0	122	1
Mp*RSL1*^{GOF3}	117	0	0	151	1
Mp*RSL1*^{GOF4}	76	0	0	97	1
Mp*RSL1*^{GOF5}	116	0	0	102	1

Table S2, related to figure S2

Mp*RSL1*^{GOF} lines allelic test.

Crosses	Plants F1 exhibiting a hairy phenotype (%)
Mp*RSL1*^{GOF3} x Mp*RSL1*^{GOF1}	100 %
Mp*RSL1*^{GOF3} x Mp*RSL1*^{GOF2}	100 %
Mp*RSL1*^{GOF3} x Mp*RSL1*^{GOF4}	100 %
Mp*RSL1*^{GOF3} x Mp*RSL1*^{GOF5}	100 %

Supplemental experimental procedures

Plant material and growth

Marchantia polymorpha growth and transformation

Takaragaike-1 (Tak-1) male and Takaragaike-2 (Tak-2) female *M. polymorpha* accessions were used in this study [S1]. Mutants grew from spores resulting from a cross between Tak-1 and Tak-2. Gemmae or meristematic segments were propagated on ½ Johnson's medium [S2] supplemented with 1% agar in Petri dishes under a 16 h light: 8 h dark photoperiod at 23°C and a light intensity of 56 µE.m^{-2}.s^{-1}. Sexual organ development was stimulated with far red light [S3, S4].

M. polymorpha sporelings and regenerating thalli were transformed following the protocols previously described [S1, S5]. After 2 days of co-cultivation with agrobacterium GV3301 carrying the pCambia1300, or Os*ACT1*$_{pro}$:Mp*RSL1* binary vector, transformed sporelings or regenerating thalli were selected on Johnson's medium supplemented with cefotaxime 100 µg.ml^{-1} and hygromycin 10 µg.ml^{-1} or gentamycin 100 µg.ml^{-1}.

Physcomitrella patens

Gransden wild type and Pp*rsl1* Pp*rsl2* [S6] double mutant plants were propagated in Petri dishes on KNOPS medium supplemented with 0.7% Agar under a 16 h light: 8 h dark photoperiod at 23°C and a light intensity of 56 µE.m^{-2}.s^{-1}.

Arabidopsis thaliana growth and transformation

Col-0 and At*rhd6-3* At*rsl1-1* double mutant [S6] plants were grown on soil: 2/3 of peat-based compost (Levington M2), 1/3 of vermiculite medium (Sinclair). For phenotypic analysis,

seeds were surface sterilized with a 70% Ethanol 0.1% Triton solution for 5 minutes followed by 99% ethanol solution for 5 minutes and grown as previously described [S6].

At*rhd6-3* At*rsl1-1 Arabidopsis* plants were transformed with agrobacterium GV3301 carrying *35S$_{pro}$*:Mp*RSL1* binary vector using the floral-dip method. Transformants were then selected on MS medium supplemented with 1% agar and 50 µg.ml^{-1} of hygromycin.

Phenotypic analysis

Images were captured with a Leica DFC310 FX camera mounted on a Leica M165 FC microscope.

In *Physcomitrella patens*, number of axillary hairs was measured in 5 nodes of 15 gametophores from 1-month-old wild type colonies and 5 nodes of 15 gametophores from 1-month-old Pp*rsl1* Pp*rsl2* double mutant colonies.

Phylogenetic analysis

The RSL Class I and RSL class II proteins—AtRHD6 (At1g66470), AtRSL1 (At5g37800), AtRSL2 (At4g33880), AtRSL3 (At2g14760), AtRSL4 (At1g27740), AtRSL5 (At5g43175), OsRSL1 (Os01g02110), OsRSL2 (Os02g48060), OsRSL3 (Os06g30090), OsRSL4 (Os03g10770), OsRSL5 (Os03g42100), OsRSL6 (Os07g39940), OsRSL7 (Os11g41640), OsRSL8 (Os12g32400), OsRSL9 (Os12g39850), SmRSL1 (EFJ25918.1), SmRSL2 (EFJ10890.1), SmRSL3 (EFJ29938.1), SmRSL4 (EFJ25105.1), SmRSL5 (EFJ20125.1), SmbHLH103 (EFJ14254.1), SmRSL7 (EFJ36606.1), SmRSL8 (EFJ19083.1), PpRSL1 (EF156393), PpRSL2 (EF156394), PpRSL3 (EF156395), PpRSL4 (EF156396), PpRSL5 (EF156397), PpRSL6 (EF156398) and PpRSL7 (EF156399)—from *Arabidopsis thaliana* (At), *Oryza sativa* (Os), *Selaginella moellendorffii* (Sm) and *Physcomitrella patens* (Pp) were retrieved from public databases following a published classification [S7]. MpRSL1

(KT633827), MpRSL2 (KT633828), were isolated then cloned. AtHEC2 (AT3G50330) was retrieved from NCBI database and used to root the tree. Alignment of bHLH domains from RSL Class I, RSL Class II and AtHEC2 proteins was performed with MAFFT (http://mafft.cbrc.jp/alignment/software/) and manually edited with bioedit (https://www.bioedit.com/). A maximum likelihood phylogenetic analysis was carried out on the sequence alignment using the LG model of amino acid [S8] and a Shimodaira-Hasegawa-like approximate ratio test [S9] with the program PhyML 3.0 [S10] (http://atgc.lirmm.fr/phyml/). The resulting tree was edited with the program figtree (http://tree.bio.ed.ac.uk/software/figtree/).

Generation of Os*ACT1pro:*Mp*RSL1* and *35Spro:MpRSL1*.

35S$_{pro}$-GW has been generated by inserting a Gateway cassette into the *Cla*I restriction site of pCambia1300a vector containing a 35S promoter and a Nos terminator. The vector pOsAct-108-hygro [S11] has been digested with *Sma*I and *Pst*I to remove the promoter Os*ACT1*$_{pro}$. The promoter Os*ACT1*$_{pro}$ was then subcloned into pCambia1300a previously digested with *Eco*RI and *Pst*I. Then, the resulting vector was digested with *Xba*I and *Hin*dIII to remove the cassette Os*ACT1*$_{pro}$:*Pst*I:Term. This cassette was then placed into the vector pMpGW207 containing gentamycin resistance [S12] previously digested with *Sac*I and *Hin*dIII. Os*ACT1*$_{pro}$-GW-Term has been obtained by insertion of a gateway cassette into the *Pst*I restriction site. Full length cDNA of Mp*RSL1* was amplified with specific primers (See the list of primers sequences below) and cloned into pCR8-GW pTOPO (Invitrogen). A subsequent LR reaction allowed the insertion of full length cDNA into pOs*ACT1*$_{pro}$-GW or *35S*$_{pro}$-GW vector to generate Os*ACT1*$_{pro}$:Mp*RSL1* and *35S*$_{pro}$:Mp*RSL1*.

Molecular analysis of mutants

Genomic DNA extraction

Genomic DNA was isolated from 1-month-old plants grown in sterile conditions. Tissues were ground in liquid nitrogen and the DNA was extracted with 2% cetyltrimethyl ammonium bromide (CTAB) buffer as previously described [S13].

Identification of DNA sequences flanking T-DNA insertions

Tail PCR was performed in Mp*RSL1*^{GOF} and Mp*rsl1* lines to identify sequences flanking the T-DNA insertion. Specific primers to the T-DNA sequence (TR1 to TR3 and TL1 to TL3 for right border T-DNA and left border T-DNA respectively) and universal adaptor primers (AD1 to AD6) were used as described previously (See the list of primers sequences below) [S1, S14].

Measurement of steady state mRNA levels using quantitative RT-PCR

Total RNA was extracted from frozen tissues using a plant RNeasy plant mini kit (Qiagen) according to the manufacturer's protocol. cDNA was synthesized from 1 µg of total RNA at 42 °C for 1 h with 200 U the protoscript 2 reverse transcriptase (NEB) and 2 µM of dT17 oligonucleotides. Quantitative RT-PCR was carried on a 7300 Applied Biosystem thermocycler. Amplification reactions were performed into 10 µl volume medium containing 5 µl of 2X SYBR green mastermix (Applied Biosystem), 500 nM of each primer (See the list of primers sequences below), and 4 µl of 1:10 diluted cDNA (corresponding to 20 ng of reverse transcribed total RNA). A two-step program composed of a denaturation step at 94°C for 15 seconds and a hybridization-elongation step at 60°C for 1 minute was repeated 40 times, then, a dissociation stage was performed. The transcript levels of genes were calculated with Linreg v2012.0 [S15, S16].

Fixation and wax inclusion for laser microdissection experiments

Plants were fixed in 100% acetone for 24 h at 4°C. The samples were then incubated in 1/1 acetone with Histoclear (v/v) and a 100% histoclear solution, for 5 minutes each, then embedded in wax with Tissue Tek® VIPTM. 8 µm sections were then placed on Membrane Slide 1.0 PEN (D) (#415190-9041-000, Zeiss) and dried overnight at 37°C.

Laser capture microdissection

Laser capture micro-dissection was performed on 8 µm thin sections of wax embedded specimens (see supplemental information) using a Carl Zeiss PALM microbeam microscope and PALMRobo 4.5V software driving the laser (laser power: 43, laser focus: 35, LPC delta +27, 1 cycle of cutting). Captured cells were collected in AdhesiveCap 500 clear (D) tubes (#415190-9211-000, Zeiss). RNA was extracted with Arcturus PicoPureTM RNA isolation kit (#KIT0204, Lifetechnologie) then cDNA were synthesized and amplified with Ovation RNA-Seq System v2 (#7102, NuGen) following the manufacturer's protocol. 1 µl of non-diluted amplified cDNA was used for expression analysis by PCR.

Plastic sectioning

Isolated gemmae cups from 1-month-old plants were fixed in fresh 4% paraformaldehyde in phosphate buffered saline (PBS) buffer (8 $g.L^{-1}$ of NaCl, 0.2 $g.L^{-1}$ of KCl, 1.44 $g.L^{-1}$ of NaH_2PO_4 and 0.24 $g.L^{-1}$ of KH_2PO_4) for 24 hours at 4°C. Chlorophyll was removed by incubation for 1 h in 30%, 70% and 100% ethanol. After rehydration in an ethanol series (100, 70 and 30%) for 20 minutes each, samples were placed in 1% molten agarose. Once the agarose solidified, the embedded samples were washed twice in sterile water then dehydrated in an ethanol series (30, 70 and 100%). Dehydrated samples were then embedded in Technovit® 7100 cold-polymerising resin (#14653, Kulzer) [S17]. µm) 4 µm sections were

made with an Ultracut E (Reichert-Jung). Images were taken captured with a Micropublisher 5.0 RTV (Q-Imaging) camera mounted on a Leica DMRB microscope.

Sequences of primers used in this study

Cloning

MpRSL1-ATG	ATGGCGAATTATGATAGCAGC
MpRSL1-Stop	GCAGACAACAACTCGTCCTGA

Genotyping

Primer A	ATGGGGCAAAGTCAGGGTAT
Primer B	GTGAATTCGACTTGGTGTAAG
Primer 1	CCGTAAGTCAATTAAGGAG
Primer 2	CTGTTTCCACGAACTCCTC
Primer 3	GTGGTGTGGAGGAGTCGTTG
Primer 4	CAGTATCGTATCAAGCCGAAG
Primer 5	GACCCTGATACACAATTTCGC
Primer 6	TCCGTCCACACACATTCTAGG
Primer R	GCTGGCGTAATAGCGAAGAGG
Primer L	GGTTTCGCTCATGTGTTGAGC

Tail PCR:

Primer AD1	NGTCGASWGANAWGAA
Primer AD2	TGWGNAGSANCASAGA
Primer AD3	AGWGNAGWANCAWAGG
Primer AD4	GTNCGASWCANAWGTT
Primer AD5	NTCGASTWTSGWGTT
Primer AD6	WGTGNAGWANCANAGA
Primer TR1	CCTGCAGGCATGCAAGCTTGG

Primer TR2	GCTGGCGTAATAGCGAAGAGG
Primer TR3	CCTGAATGGCGAATGCTAGAG
Primer TL1	CAGATAAGGGAATTAGGGTTCCTATAGG
Primer TL2	TATAGGGTTTCGCTCATGTGTTGAGC
Primer TL3	AGTACATTAAAAACGTCCGCAATGTG

Gene expression:

MpRSL1-F	AGATGAGTCTGGGGCAACC
MpRSL1-R	GGATGAGCGCTTTAGAGTG
MpEF1-F	CCGAGATCCTGACCAAGG
MpEF1-R	GAGGTGGGTACTCAGCGAAG
MpCUL1-F	AGGATGTGGACAAGGATAGACG
MpCUL1-R	GTTGATGTGGCAACACCTTG
MpACT-F	AGGCATCTGGTATCCACGAG
MpACT-R	ACATGGTCGTTCCTCCAGAC
AtRHD6-F	CCTAAATCCGCTGGAAACAA
AtRHD6-R	CTCTTGGATTCTTGGCTGCT
AtRSL1-F	CCCTAAACTGGCTGGCAATA
AtRSL1-R	TCTTGGCTGCTAGGCTTTGT
AtUBQ-F	GGCCTTGTATAATCCCTGATGAATAAG
AtUBQ-R	AAAGAGATAACAGGAACGGAAACATAGT

Supplemental references

S1. Ishizaki, K., Chiyoda, S., Yamato, K.T., and Kohchi, T. (2008). Agrobacterium-mediated transformation of the haploid liverwort *Marchantia polymorpha* L., an emerging model for plant biology. Plant Cell Physiol. *49*, 1084-1091.

S2. Johnson, C.M., Stout, P.R., Broyer, T.C., and Carlton, A.B. (1957). Comparative chlorine requirements of different plant species. Plant and Soil *8*, 337-353.

S3. Fredericq, H., and De Greef, J. (1966). Red (R), far-red (FR) photoreversible control of growth and chlorophyll content in light-grown thalli of *Marchantia polymorpha L*. Naturwissenschaften *53*: 337.

S4. Wann, F. (1925). Some of the factors involved in the sexual reproduction of *Marchantia polymorpha*. Am. J. Bot. *12*: 307–318.

S5. Kubota, A., Ishizaki, K., Hosaka, M., and Kohchi, T. (2013). Efficient Agrobacterium-mediated transformation of the liverwort *Marchantia polymorpha* using regenerating thalli. Bioscience, Biotechnology, and Biochemistry 77, 167-172.

S6. Menand, B., Yi, K., Jouannic, S., Hoffmann, L., Ryan, E., Linstead, P., Schaefer, D.G., and Dolan, L. (2007). An ancient mechanism controls the development of cells with a rooting function in land plants. Science *316*, 1477-1480.

S7. Pires, N., and Dolan, L. (2010). Origin and diversification of basic-helix-loop-helix proteins in plants. Mol. Biol. Evol. *27*, 862-874.

S8. Le, S.Q., and Gascuel, O. (2008). An improved general amino acid replacement matrix. Mol. Biol. Evol. 25, 1307-1320.

S9. Anisimova, M., and Gascuel, O. (2006). Approximate likelihood-ratio test for branches: A fast, accurate, and powerful alternative. Syst. Biol. *55*, 539-552.20

S10. Guindon, S., Dufayard, J-F., Lefort, V., Anisimova, M., Hordjik, V., and Gascuel, O. (2010). New algorithms and methods to estimate maximum-likelihood phylogenies: assessing the performance of PhyML 3.0. Syst. Biol. *59*, 307-321.

S11. Proust, H., Hoffmann, B., Xie, X., Yoneyama, K., Schaefer, D.G., Yoneyama, K., Nogué, F., and Rameau, C. (2011). Strigolactones regulate protonema branching and

act as a quorum sensing-like signal in the moss *Physcomitrella patens*. Development *138*, 1531-1539.

S12. Ishizaki, K., Nishihama, R., Yamato, K.T., and Kohchi, K. (2015). Molecular Genetic Tools and Techniques for *Marchantia polymorpha* Research. Plant and Cell Physiology *0*, 1-9.

S13. Porebski, S., Bailey, L.G., and Baum, B.R. (1997). Modification of a CTAB DNA extraction protocol for plants containing high polysaccharide and polyphenol components. Plant Mol. Biol. Rep. *15*, 8-15.

S14. Nelson, A. D., Lamb, J.C., Kobrossly, P.S., and Shippen, D.E. (2011). Parameters affecting telomere-mediated chromosomal truncation in Arabidopsis. Plant Cell *23*, 2263-2272.

S15. Ruijter, J.M., Ramakers, C., Hoogaars, W.M.H., Karlen, Y., Bakker, O., van den Hoff, M.J.B., and Moorman, A.F.M. (2009). Amplification efficiency: linking baseline and bias in the analysis of quantitative PCR data. Nucleic Acids Res. *37*, e45.

S16. Ramakers, C., Ruijter, J.M., Deprez, R.H., and Moorman, A.F. (2003). Assumption-free analysis of quantitative real-time polymerase chain reaction (PCR) data. Neurosci. Lett. *339*, 62-66.

S17. Jang, G., and Dolan, L. (2011). Auxin promotes the transition from chloronema to caulonema in moss protonema by positively regulating *PpRSL1*and *PpRSL2* in *Physcomitrella patens*. New Phytol. *192*, 319-327.